

Figure 1

Accepted for publication

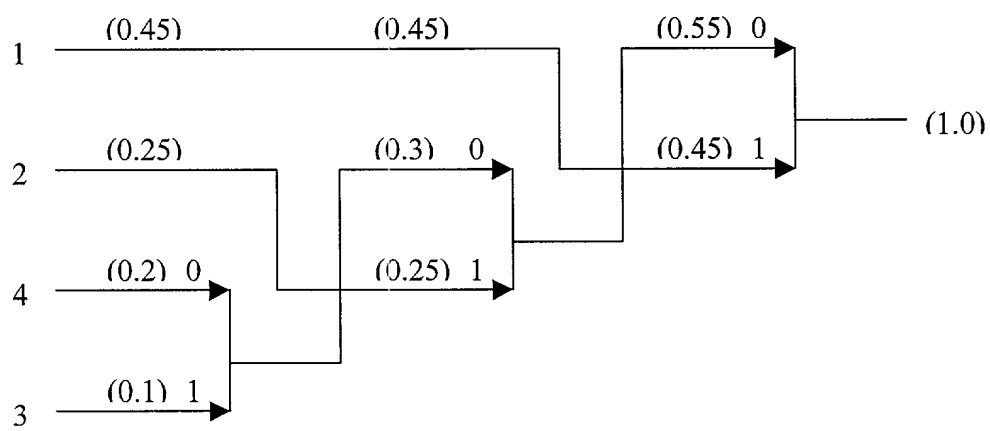


Figure 2A

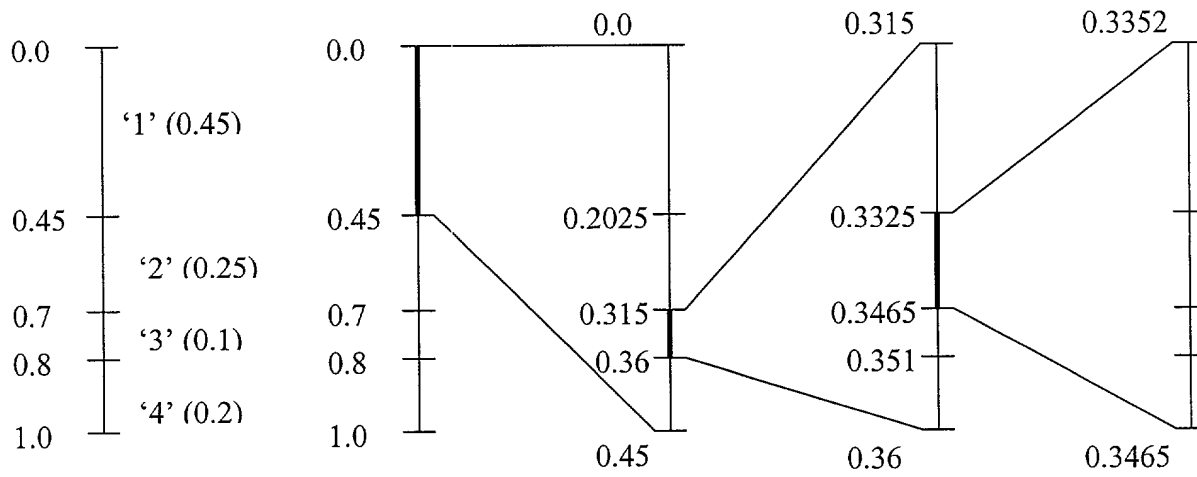


Figure 2B

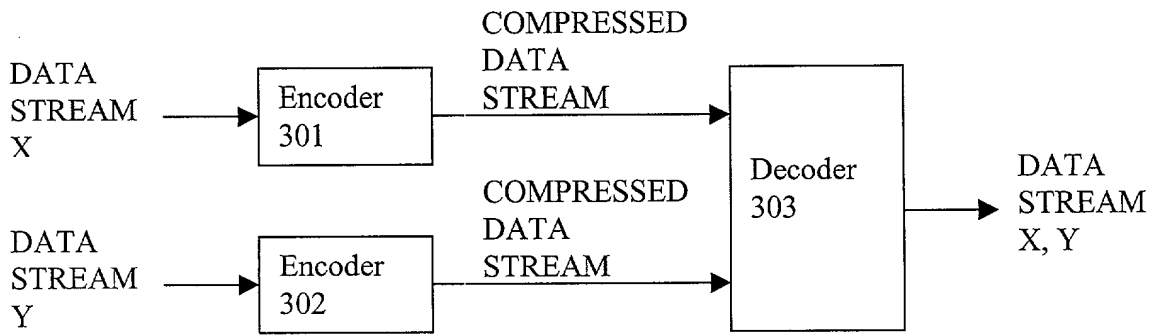


Figure 3A

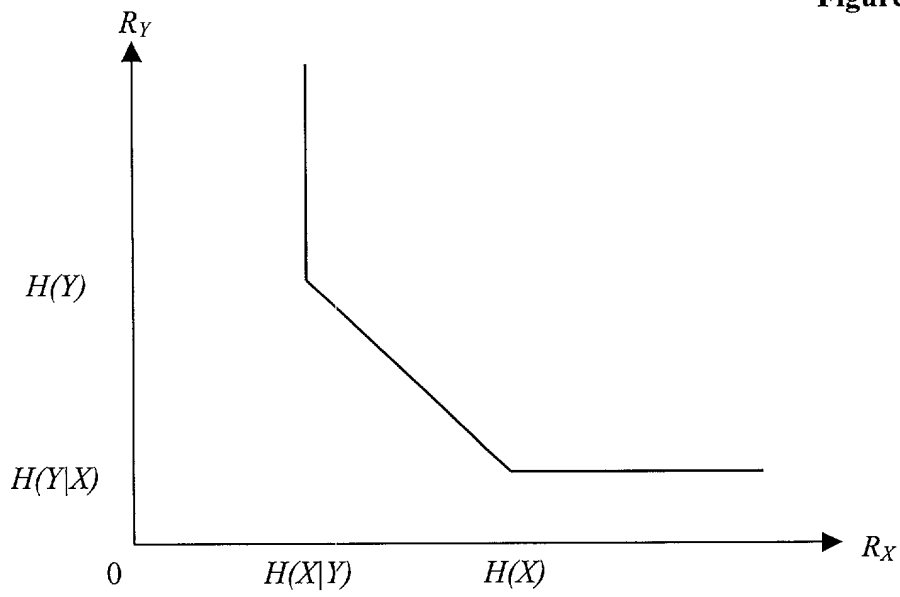


Figure 3B

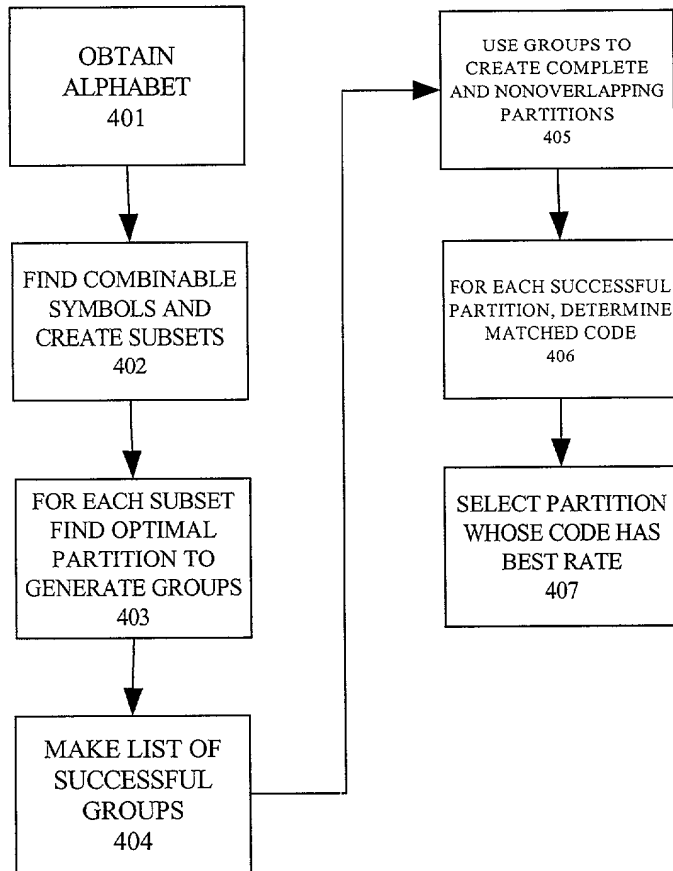


FIGURE 4

FIGURE 5

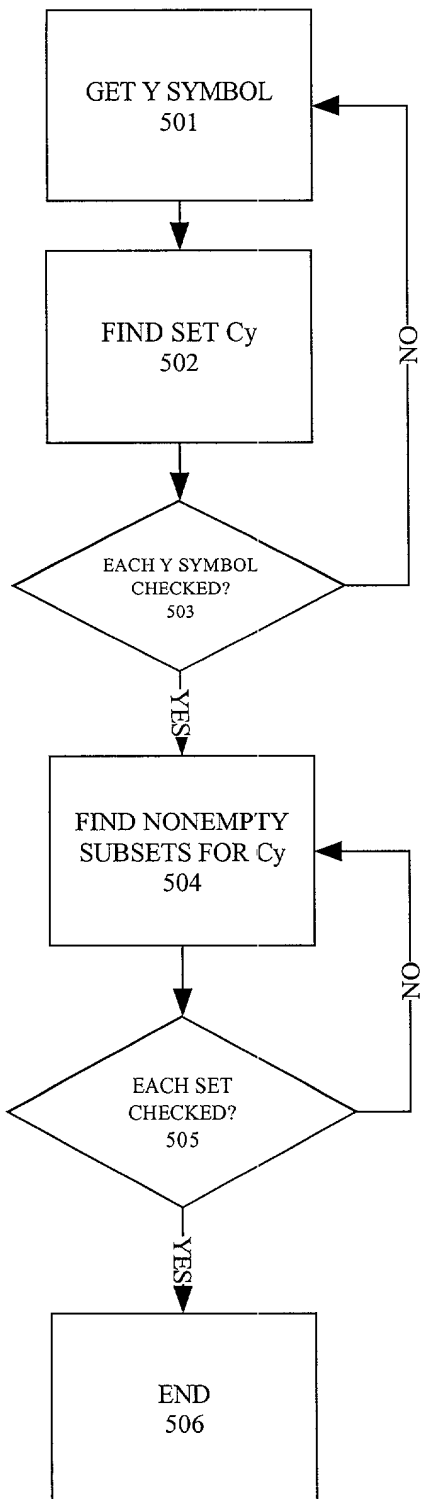


FIGURE 6

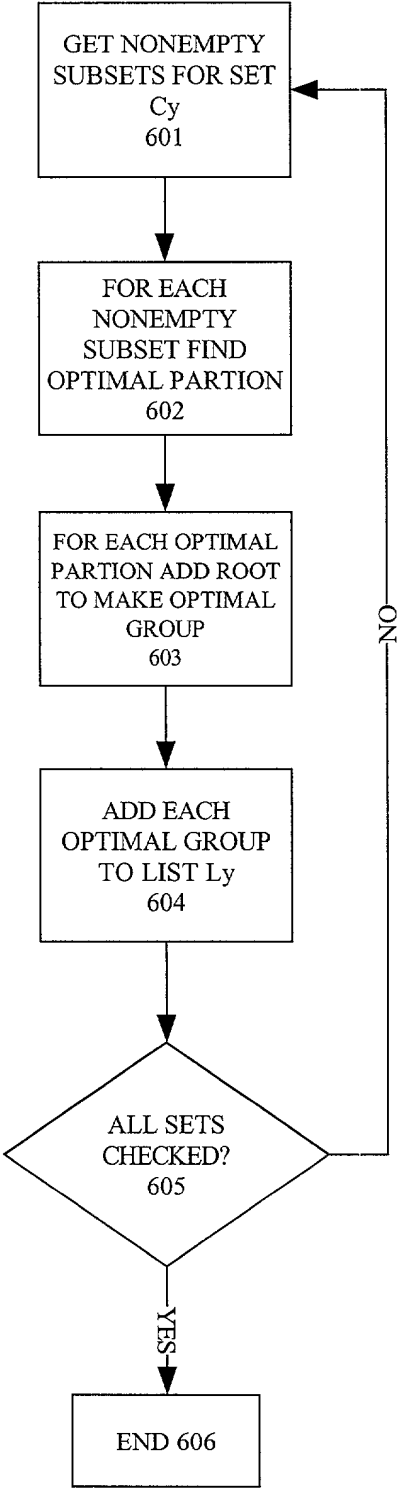
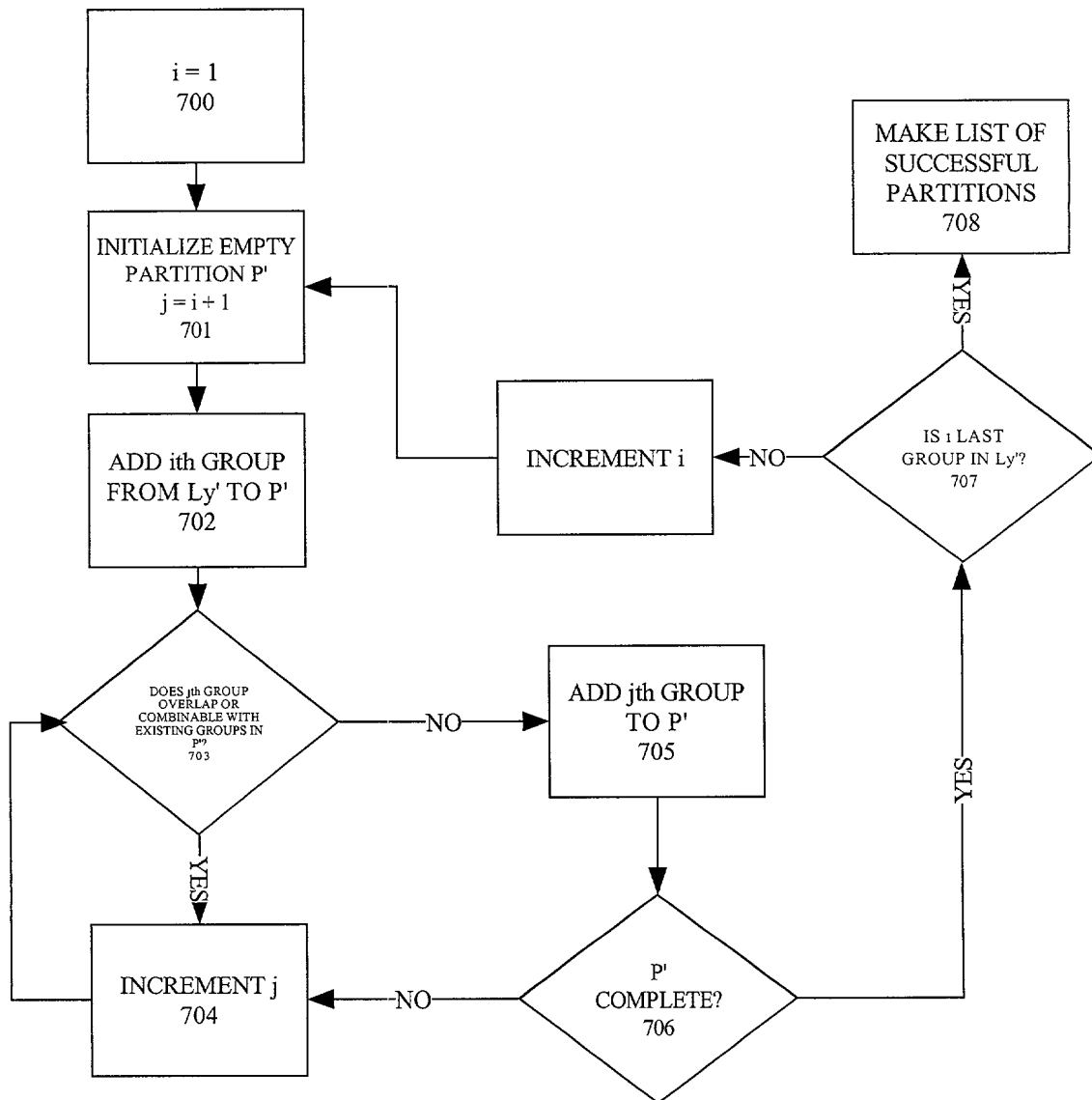


FIGURE 7



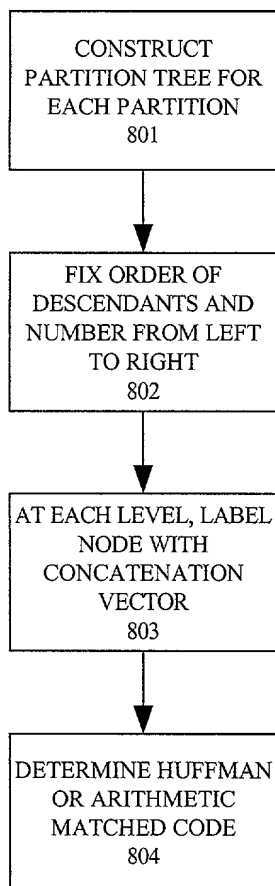


FIGURE 8

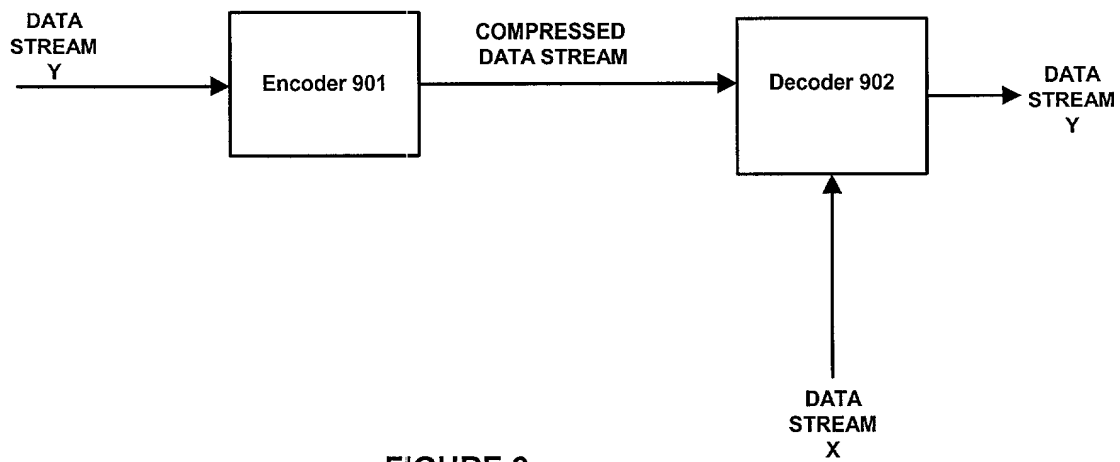


FIGURE 9

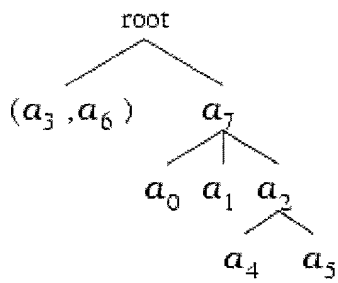


FIGURE 10A

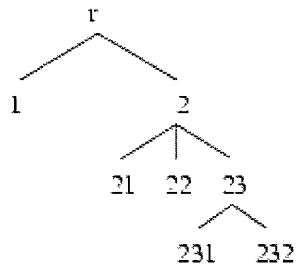


FIGURE 10B

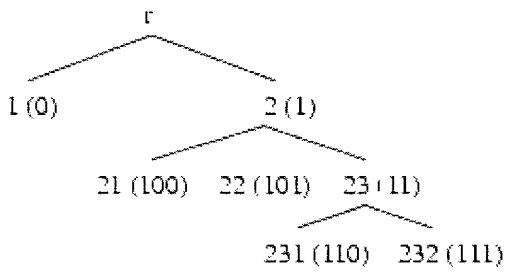


FIGURE 10C

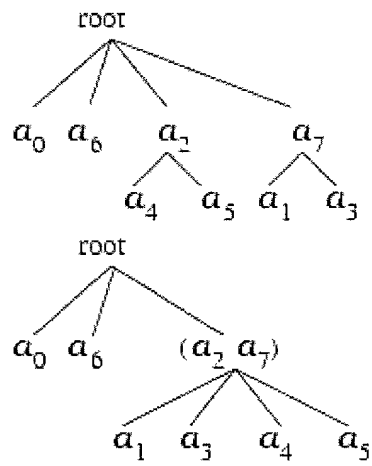


FIGURE 10D

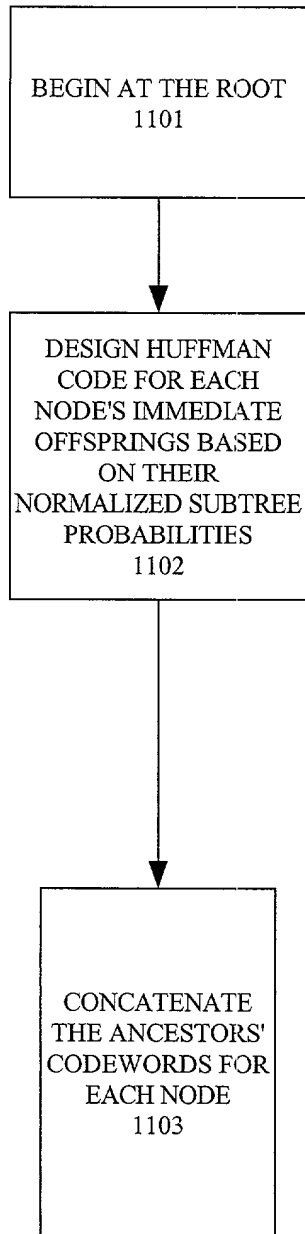


FIGURE 11

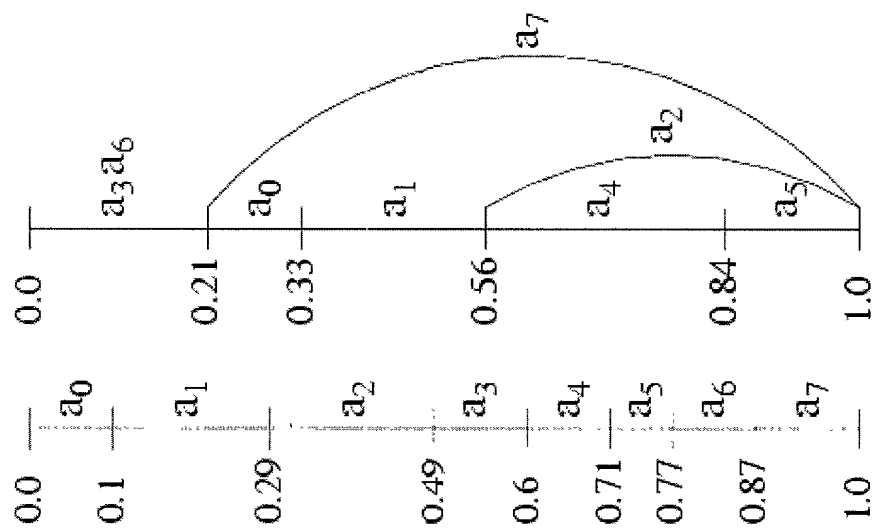


FIGURE 12A

FIGURE 12B

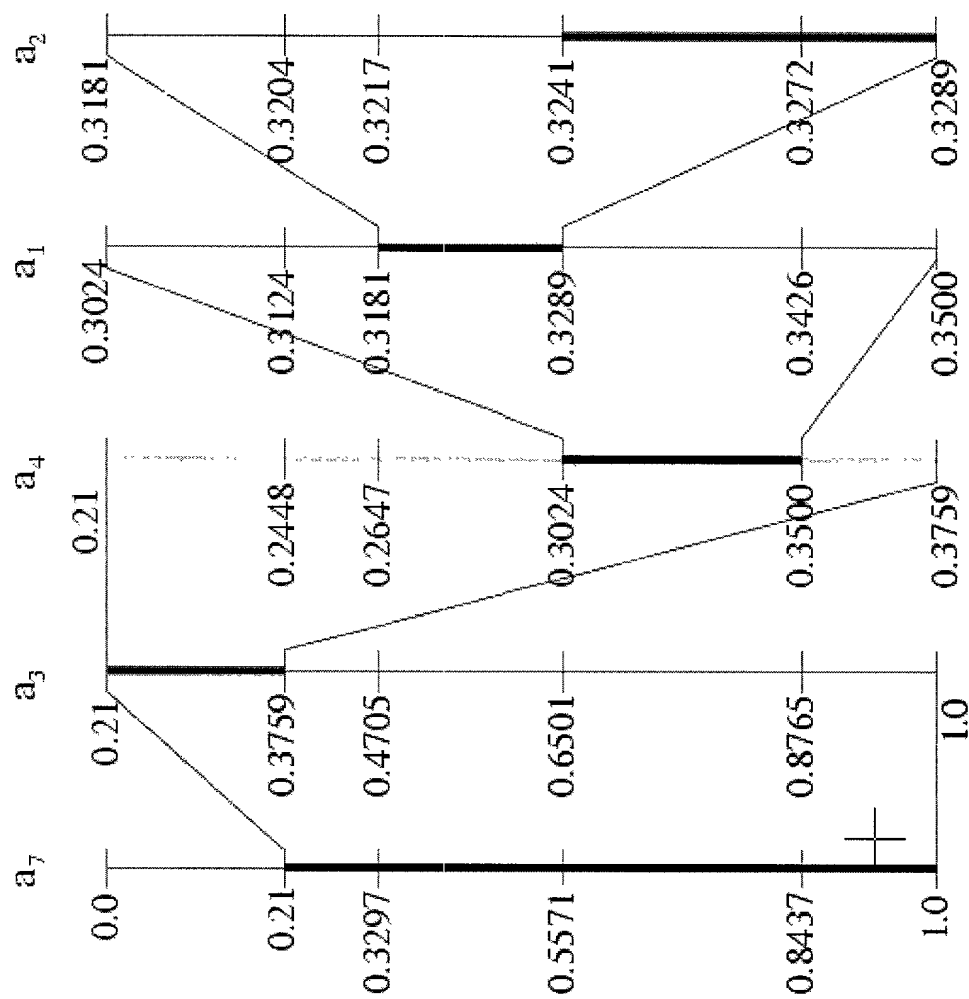


FIGURE 12C

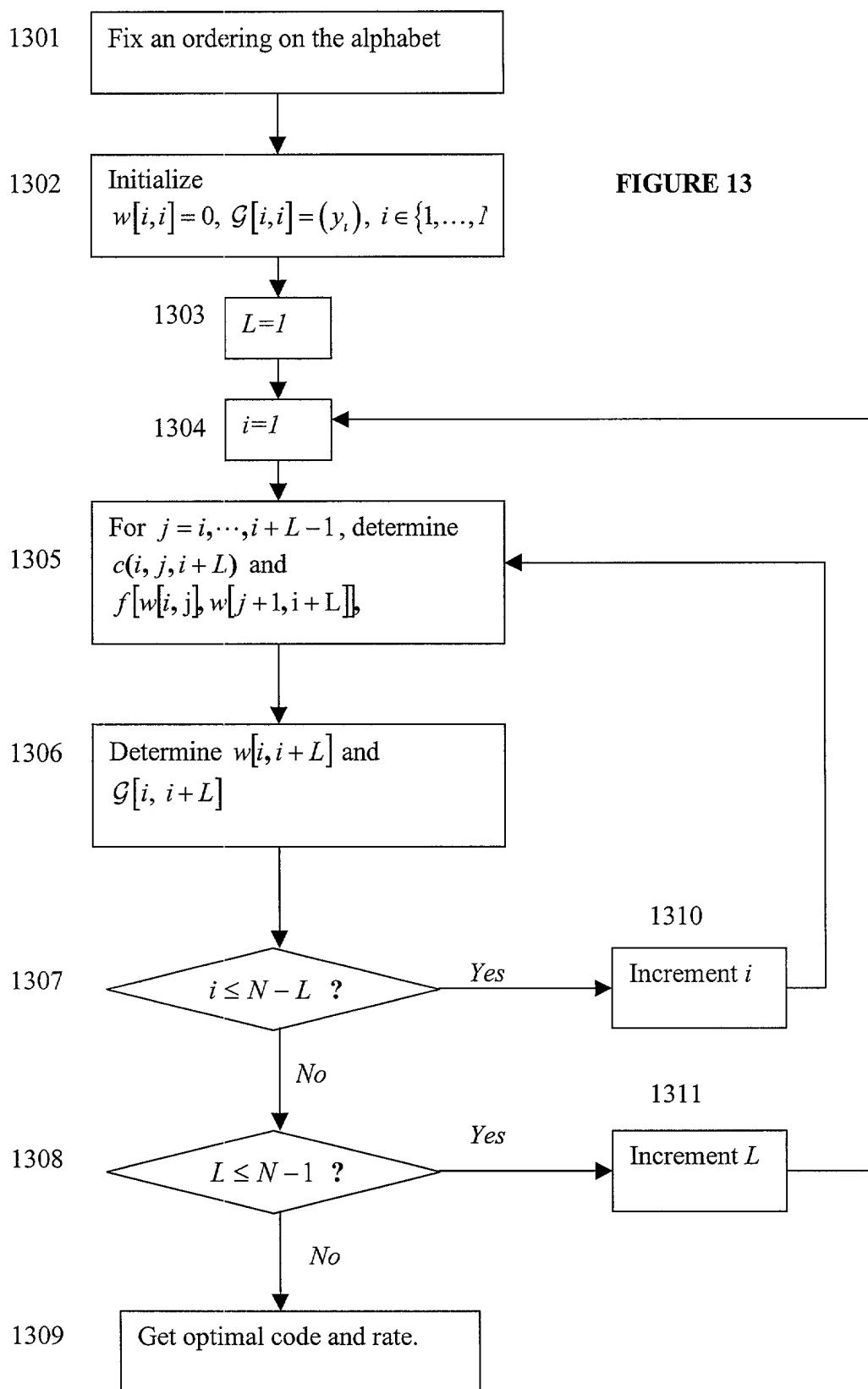
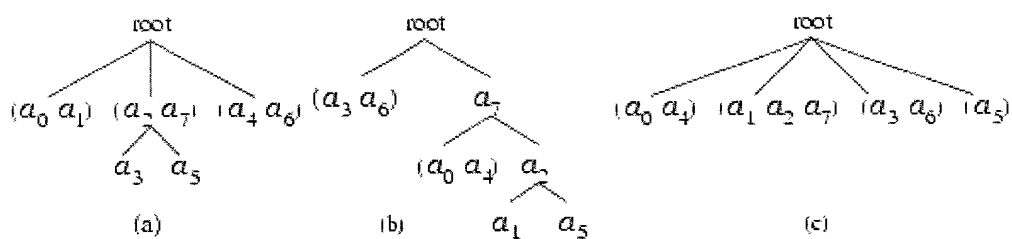
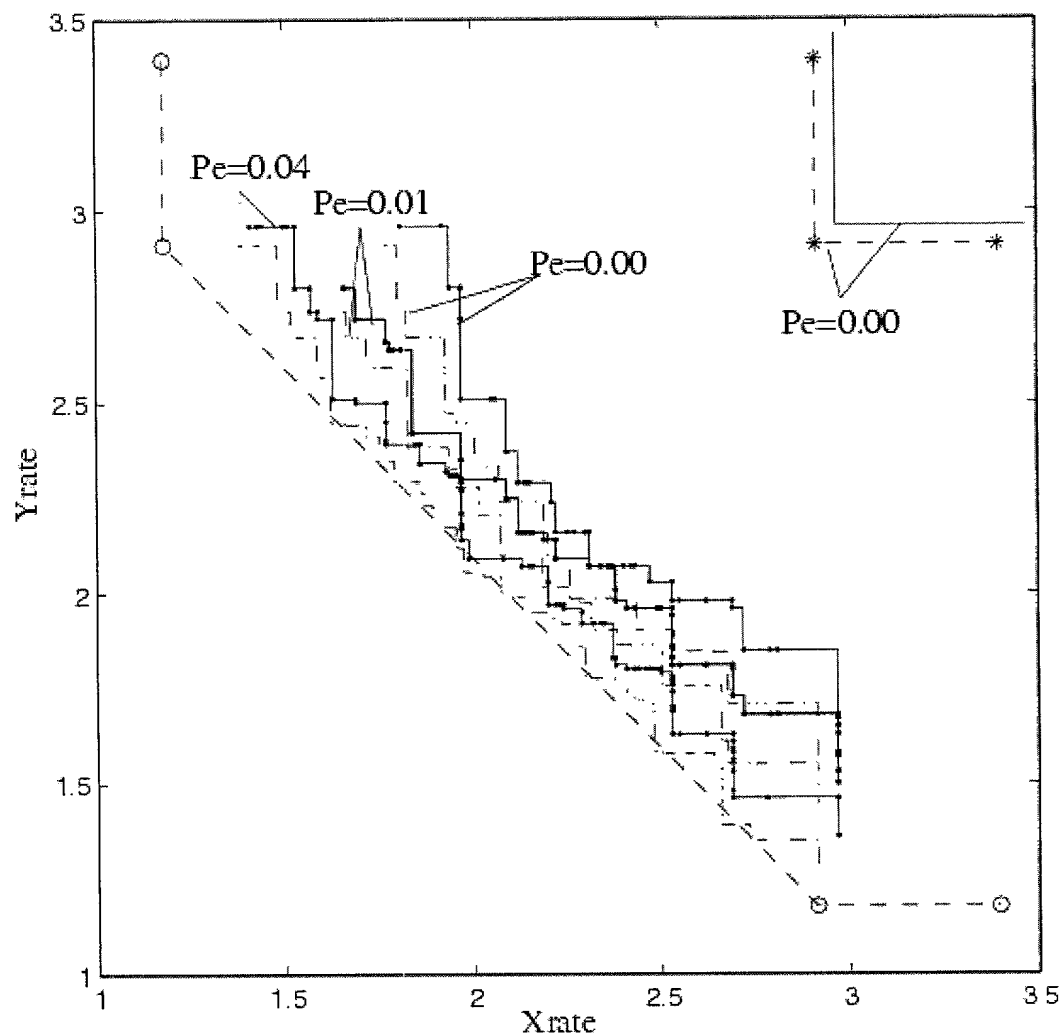


FIGURE 13



Partition trees for (a) $R_{SI,H}^*(Y)$; (b) $R_{SI,A}^*(Y)$; (c) $R_{SI,A}'(Y)$ and $R_{SI,H}'(Y)$.

FIGURE 14



MASC: code built by our algorithm

—•—•—•— MASC with Huffman coding ($n=1$)

— MASC optimal performance

⊖ ⊖ ⊖ ⊖ Slepian-Wolf rate region

IND: decode X and Y independently

— IND with Huffman coding ($n=1$)

* * * * * IND optimal performance

FIGURE 15 General lossless and near-lossless MASC results.

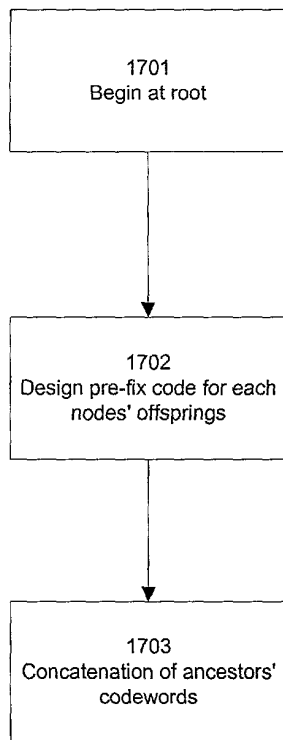


FIGURE 17

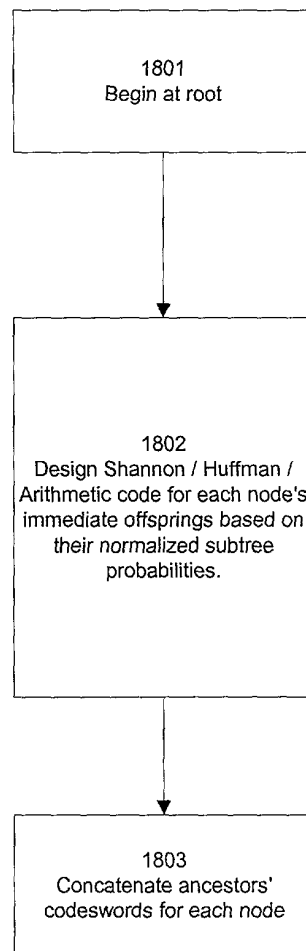


FIGURE 18